

Matching collapse and expansion across Matter Trapping surfaces in inhomogeneous Λ CDM models

Alan Maciel,^{1,*} M. Le Delliou,^{2,3,4,†} and José P. Mimoso^{5,‡}

¹*Centro de Matemática, Computação e Cognição, Universidade Federal do ABC,
Avenida dos Estados 5001, CEP 09210-580, Santo André, São Paulo, Brazil*

²*Institute of Theoretical Physics & Research Center of Gravitation, Lanzhou University, Lanzhou 730000, China
-Key Laboratory of Quantum Theory and Applications of MoE, Lanzhou University, Lanzhou 730000, China
-Lanzhou Center for Theoretical Physics & Key Laboratory of Theoretical Physics of Gansu Province, Lanzhou University, Lanzhou 730000, China*

³*Instituto de Astrofísica e Ciências do Espaço, Universidade de Lisboa,
Faculdade de Ciências, Ed. C8, Campo Grande, 1769-016 Lisboa, Portugal*

⁴*Université de Paris-Cité, APC-Astroparticule et Cosmologie (UMR-CNRS 7164), F-75006 Paris, France.*

⁵*Departamento de Física and Instituto de Astrofísica e Ciências do Espaço,
Faculdade de Ciências da Universidade de Lisboa,
Campo Grande, Ed. C8 1749-016 Lisboa, Portugal*

In previous works, Matter Trapping Surfaces (MTS) were defined as hypersurfaces separating cosmologically expanding regions of spacetime from regions where collapse can take place independently. In the present work we examine the MTS, for the restriction to spherical dust plus Λ , proving that it actually is a characteristic surface of the Cauchy problem (generated by its characteristic curves), which opens the possibility for infinite solutions. This translates as the MTS being a boundary between arbitrarily independent solutions, reminiscent of the Birkhoff theorem effects. This property is illustrated with combinations of 3 examples containing MTSs and Λ (Λ CDM, Schwarzschild-de Sitter, Lemaître-Tolman-Bondi-de Sitter: LTBDs – i.e. the inhomogeneous, spherically symmetric Λ CDM). The LTBDs model presents a static, stable MTS for the first time.

* alan.silva@ufabc.edu.br; ORCID: 0000-0002-1919-2140

† delliou@lzu.edu.cn, Morgan.LeDelliou.IFT@gmail.com; ORCID: 0000-0003-3655-2547

‡ jpmimoso@fc.ul.pt, jpmimoso@ciencias.ulisboa.pt; ORCID: 0000-0002-9758-3366

I. INTRODUCTION

The initial data problem formulation of General Relativity (GR) is the key to interpret what seems a purely geometric theory into a well defined physical theory that dictates the evolution of an admissible system. Since in GR what constitutes an initial instant is not uniquely defined, we deal with a Cauchy problem, where the conditions are imposed on spacelike hypersurfaces.

In previous works [1–3], we defined the concept of Matter Trapping Surfaces (MTS), which are dynamically defined in spherically symmetric spacetimes as surfaces that separate the regions of expansion and contraction of the spacetime. The MTS indicates the emergence of a bound region where the dynamics is decoupled from cosmological expansion, determining the frontier between the dominance of global and local physics.

This distinction is relevant for many astrophysical and cosmological fundamental questions. For instance: in which regimes can Newtonian physics provide an adequate description, and when must one rely on the full machinery of General Relativity? How do overdense regions dynamically decouple from the overall expansion of the universe? The concept of MTS offers a physically motivated criterion to distinguish these opposed regimes, by objectively characterizing the transition between locally bound and globally expanding domains.

Yet an important question that needs formal clarification is whether the MTS can be used as a boundary that would entirely determine the dynamics on each side in well posed form. This would be the case if the Einstein's Field Equations (EFEs) together with the MTS can be recast as a Cauchy problem.

As widely appreciated the initial value data and Cauchy problem are questions that are crucial for a well posed problem, and have attracted a great deal of interest in the field. The fundamental, and seminal works on this issue can be traced back to the works of Y. Choquet-Bruhat [4, 5], A. Lichnérowicz [6, 7], S. Deser [8], and J. W. York [9–12]. Other works have made relevant contributions in connection to particular aspects of this endeavour [13–17], and a few enlightening reviews provide a thorough overview of the numerous contributions, namely in what regards the main conceptual questions [18], and in what concerns the important numerical applications [19, 20].

In the present work, we impose boundary conditions on the MTS, assuming a matter content composed of dust and a cosmological constant. The result is that, in this case, the MTS corresponds to a characteristic surface in the Cauchy sense, implying that the evolution on each side of this surface is completely decoupled. This means that, apart from physical considerations regarding the continuity of certain quantities such as mass-energy, any interior solution can be matched with any exterior solution across an MTS. This characterizes the MTS not only as a separating surface between regions of expansion and collapse, but also as a shield that protects each side from the detailed dynamics of the other. The only physical variables that each side perceives from the other are the averaged quantities that must be matched at the MTS to ensure continuity.

An outline of the work is as follows,. In Sec. II, we introduce the formal tools that we shall use in the subsequent analysis of the Cauchy problems, namely the 1+1+2 spacetime splitting, its translation into the GPG line element vocabulary and the MTS characterisation. We focus on the Λ -CDM model (i.e. Λ plus dust model) that is now favoured by observations and is somewhat the present standard model of cosmology. In this very same section we develop our analysis of the MTS as a Cauchy problem. In Sec. III we illustrate our results considering some particular realizations of scenarios where the MTS separates two different solutions. We envisage Schwarzschild-de Sitter matching, the Einstein-de Sitter model, and we build a more evolved model where there is a sigmoid-like transition between two Lemaître-Tolman-Bondi solutions motivated by Large-Scale-Structure (LSS) models. Finally in Sec. IV we conclude and provide final remarks discussing our results.

II. THE MTS AS A CAUCHY PROBLEM FOR DUST WITH Λ

We recall the extended Lemaître-Tolman-Bondi (LTB) model, presenting a spherically symmetric content of dust and a cosmological constant, approached as a perfect fluid combination. The dust with Λ case corresponds to the Λ CDM model presently favoured by cosmology, and hence presents an interest on its own [21]. In this setting we consider the MTS as a limit surface, and we study the possibility of integrating spacetime from boundary data given on the MTS towards each side. That is, investigating each side of the MTS to ascertain whether it can be identified as a Cauchy surface for the PDE system given by Einstein field equations (EFE) in this setup.

A. From 1+1+2 to GPG

The 1+1+2 formalism applied to spherically symmetric metrics consists in choosing a timelike future directed unit vector n^a along the matter flow, and a unit spacelike vector e^a orthogonal to n^a and the spheres of symmetry. The metric can be written as:

$$g_{ab} = -n_a n_b + e_a e_b + N_{ab}, \quad (1)$$

where N_{ab} correspond to the induced 2-metric on the spheres of symmetry. By introducing the areal radius r , we can write $N_{ab} = r^2 \Omega_{ab}$ where Ω_{ab} is the metric of the unit 2-sphere.

In order to study the dynamics of those spacetimes we resort to the use of geometrical scalars defined from those quantities, namely, the 2-expansions Θ_n and Θ_e defined, when the areal radius can be defined, as

$$\Theta_n = \frac{2}{r} \mathcal{L}_n r, \quad (2)$$

$$\Theta_e = \frac{2}{r} \mathcal{L}_e r. \quad (3)$$

In general we can define Θ_X for any X^a in the (n^a, e^a) plane by the same formula. The interest here is to relate this approach with the well known GPG coordinates. In order to achieve this goal, we recall the definition of the Misner-Sharp mass-energy M_{ms} [22, hereafter MS]:

$$g^{ab} \partial_a r \partial_b r = 1 - \frac{2M_{ms}}{r}, \quad (4)$$

which, together with Eq. (1), gives us

$$-(n^a \partial_a r)^2 + (e^b \partial_b r)^2 = 1 - \frac{2M_{ms}}{r}, \quad (5)$$

as the areal radius gradient is orthogonal to the 2-spheres. We may rearrange it as

$$e^b \partial_b r = \pm \sqrt{1 + (n^a \partial_a r)^2 - \frac{2M_{ms}}{r}}. \quad (6)$$

We interpret the term $n^a \partial_a r$ as the fluid radial velocity $\frac{dr}{d\tau}$. We are then motivated to define

$$E = (n^a \partial_a r)^2 - \frac{2M_{ms}}{r}, \quad (7)$$

which corresponds to twice the Newtonian mechanic energy per unit mass¹.

Using the scalar function E , Eq. (6) becomes

$$e^b \partial_b r = \pm \sqrt{1 + E}. \quad (8)$$

The GPG coordinates correspond to using a timelike coordinate t chosen along the flow, along with the areal radius as the spacelike coordinate orthogonal to the spheres of symmetry. Therefore, translating from the abstract index notation to a coordinate notation we have

$$n_a dx^a = -\alpha(t, r) dt, \quad (9)$$

where we chose the $-$ sign in order to guarantee t is future directed with positive $\alpha(t, r)$, that we recognise as the shift function in the Arnowitt-Deser-Misner decomposition [23, hereafter ADM]. Since, by construction, $n_a e^a = 0$, e^a has the form $(0, e^r, 0, 0)$. By Eq. (8), we conclude that

$$e^r = \sqrt{1 + E} \Rightarrow e^a \partial_a = \sqrt{1 + E(t, r)} \partial_r, \quad (10)$$

¹ In some sources E is defined as the Newtonian energy per unit mass, but here we prefer to avoid a factor 2 appearing in the GPG metric.

where we chose the + sign in order to direct e^a outwards, that is, in the direction of increasing r .

In order to translate the full metric into coordinate notation we have to find the form of e_a . Since e^a is a unit vector, applying $e^a e_a = 1$ gives us $e_a = (e_t, \frac{1}{\sqrt{1+E}}, 0, 0)$, with e_t unconstrained. Therefore, by defining a function $\beta(t, r) = -e_t \sqrt{1+E}$, such that it is positive for outwards flow, we write:

$$e_a dx^a = \frac{1}{\sqrt{1+E(t, r)}} (-\beta(t, r) dt + dr) . \quad (11)$$

Plugging Eqs. (9) and (11) into Eq. (1) and making the final translation

$$N_{ab} \partial_a \partial_b = r^2 (d\theta^2 + \sin^2 \theta^2 d\varphi^2) = r^2 d\Omega^2 , \quad (12)$$

we obtain the well known GPG line element [24–28] :

$$ds^2 = -\alpha(t, r)^2 dt^2 + \frac{(-\beta(t, r) dt + dr)^2}{1 + E(t, r)} + r^2 d\Omega^2 . \quad (13)$$

In order to interpret the meaning of $\beta(t, r)$, we compute n^a in GPG coordinates

$$n^a \partial_a = \frac{1}{\alpha(t, r)} (\partial_t + \beta(t, r) \partial_r) , \quad (14)$$

which gives us

$$n^a \partial_a r = \frac{\beta(t, r)}{\alpha(t, r)} , \quad (15)$$

and therefore relates β with the fluid areal radial velocity.

Thus the lapse function $\alpha(t, r)$ regulates the evolution between adjacent hypersurfaces, while the shift vector $\beta(t, r) \partial_r$ corrects point to point for the flow so that the radial coordinate remains the areal radius r .

B. Dynamical Equations

We consider the perfect fluid case, and formulate the Einstein field equations in terms of the Misner-Sharp mass M_{ms} , and of the energy function E , respectively defined in (4) and (7). This allows us to single out the MTS in a way that makes clear how it constrains the matter flow, before recasting the dynamical equations in Cauchy form for the restriction to dust and Λ . The solution may be given associating M_{ms} with the cosmological constant and perfect fluid masses, and introducing the contribution of the cosmological constant at the level of the shift solution.

Choosing n^a as the fluid rest observer 4-velocity,² the energy-momentum tensor of a perfect fluid is

$$T_{ab} = \rho n_a n_b + P(e_a e_b + N_{ab}) . \quad (17)$$

where ρ and P respectively are the energy-density and the pressure of the fluid as measured by the co-moving observer.³

² Note the usual flow-orthogonal projector h_{ab} becomes

$$h_{ab} \equiv g_{ab} + n_a n_b = e_a e_b + N_{ab} , \quad (16)$$

and we can also interpret the 2-metric N_{ab} as being the projector onto the subspace orthogonal to both n^a and e_a .

³ In the case when the fluid is also admitting anisotropic stress [3], the energy momentum tensor reads

$$T_{ab} = \rho n_a n_b + P(e_a e_b + N_{ab}) + \Pi_{ab} . \quad (18)$$

In spherical symmetry, the anisotropic stress reduces to $\Pi_{ab} = \Pi(N_{ab} - N_c^c e_a e_b)$. The perfect fluid case then corresponds to $\Pi_{ab} = 0$. A cosmological constant can be modeled as a perfect fluid with $\rho = -P = \frac{\Lambda}{8\pi}$ [see, e.g. 29, p172].

The Einstein Field Equations (EFEs) can then be written

$$\dot{E} + \beta \left(E' + \frac{2(1+E)}{\rho+P(\rho)} \frac{dP}{d\rho} \rho' \right) = 0, \quad (19a)$$

$$\dot{M}_{ms} + \beta (M'_{ms} + 4\pi P(\rho)r^2) = 0, \quad (19b)$$

$$M'_{ms} - 4\pi r^2 \left(\rho + \frac{\Lambda}{8\pi} \right) = 0. \quad (19c)$$

$$\frac{\alpha'}{\alpha} + \frac{P'}{\rho+P} = 0. \quad (19d)$$

where M_{ms} includes both the contribution of the perfect fluid and that of the cosmological constant, i.e,

$$M_{ms} = M + \frac{\Lambda}{6}r^3. \quad (20)$$

with $M = 4\pi \int_0^r \rho(u', t = t_0) u^2 du$ representing the total spherical mass-energy of the perfect fluid contained in a given radius, in spherical symmetry. They are to be complemented with an equation of state of the form

$$f(\rho, P) = 0. \quad (21)$$

Note that the solution, with the perfect fluid energy density ρ and isotropic pressure P , can be expressed in terms of E , the energy/curvature of the spatial hypersurfaces, and of the Misner-Sharp mass, M , of the fluid. Given that in the case of multiple fluids, the various corresponding masses, densities and pressures are summed, and that the energy/curvature results from the total mass sum, we find for β

$$\beta(t, r) = \pm \alpha(t, r) \sqrt{\frac{2M(t, r)}{r} + \frac{\Lambda r^2}{3} + E(t, r)}, \quad (22)$$

where the $-$ sign corresponds to collapse and the $+$ sign, to expansion⁴.

The system is closed by the following data given on the initial $t = t_0$ hypersurface:

$$\rho(t_0, r) = g(r), \quad (23a)$$

$$\dot{\rho}(t_0, r) = h(r). \quad (23b)$$

In Ref. [1] a separating surface that we named Matter Trapping Surface (MTS) was defined by the following conditions⁵

$$\mathcal{L}_n r = 0, \quad (25a)$$

$$\mathcal{L}_n (\mathcal{L}_n r) = 0, \quad (25b)$$

and hence $\Theta_n = \mathcal{L}_n \Theta_n = 0$ according to Eq. (2).

In terms of the integral quantities E and $M_{ms} = M + (\Lambda/6)r^3$ the MTS conditions read

$$E = -\frac{2M}{r} - \frac{\Lambda r^2}{3}, \quad (26a)$$

$$\text{gTOV} \equiv \frac{M}{r^2} - \frac{\Lambda r}{3} + 4\pi r P + \frac{1+E}{\rho+P} P' = 0, \quad (26b)$$

where gTOV is a functional we proposed in Mimoso et al. [1] that yields the Tolman-Oppenheimer-Volkoff (TOV) equilibrium equation [30, 31] on the MTS. The first of these conditions, sets the locus of turnaround radius [32–36], and was coined the kinematic condition. It reveals that the MTS can only exist in positively curved/negative energy

⁴ Note that our definition for $\beta(t, r)$ corresponds to that in Lasky and Lun [24] with the opposite sign.

⁵ Note that these conditions can be recast in a geometric and gauge independent form, using the expansion Θ_n of the evolving 2-surface in the MTS along the flow of matter n^a , that is related to the flow volume expansion Θ_3 and to its spherical shear scalar σ by $\Theta_n = 2 \left(\frac{\Theta_3}{3} + \sigma \right)$. In spherical symmetry, $\frac{\Theta_3}{3} + \sigma = \frac{\mathcal{L}_n r}{r}$. Therefore, for $r \neq 0$, we have equivalence between the geometric expression of the MTS conditions and the gauge invariant expressions

$$\left. \begin{aligned} \mathcal{L}_n r &= \frac{r}{2} \Theta_n = 0 \\ \mathcal{L}_n \mathcal{L}_n r &= \frac{r}{2} \left(\mathcal{L}_n \Theta_n + \frac{\Theta_n^2}{2} \right) = 0 \end{aligned} \right\} \Leftrightarrow \left\{ \begin{aligned} \Theta_n &= 0, \\ \mathcal{L}_n \Theta_n &= -\frac{\Theta_n^2}{2} = 0. \end{aligned} \right. \quad (24)$$

regions. The second condition balances the radial acceleration, and may separate regions of opposite accelerations. It is named the dynamic condition, and can be related to the cracking condition first put forward by Herrera [37–39] in the framework of the gravitational instability of bound spherical distributions of matter surrounded by vacuum.

The question now that needs clarification is whether the MTS can be used as a boundary setting that would entirely determine the dynamics on each side. This would be the case if the EFEs together with the MTS can be recast as a Cauchy problem.

A Cauchy problem is defined as system of n partial differential equations in \mathbb{R}^m , of up to k -th order, in n unknown functions, with boundary/initial data given in an $m - 1$ dimensional hypersurface of \mathbb{R}^m for derivatives up to $k - 1$ -th order for each of the n unknown functions. Therefore, the system given by Eqs. (19) with the set of data (23), having unclear choice of unknown functions, is not a Cauchy problem in this form. We then have to rewrite it as an equivalent Cauchy problem in order to use some mathematical results.

C. The dust and Λ model

In the case when the perfect fluid source reduces to dust and a cosmological constant Λ , we notice at once that

$$\frac{\alpha'}{\alpha} = 0. \quad (27)$$

From Eq. (27), we see that α is only a function of time and thus we can set $\alpha = 1$ by a time rescaling in the metric (13). Thus the system of field equations is reduced to [1, 2, 24]

$$\dot{E} + \beta E' = 0, \quad (28a)$$

$$\dot{M} + \beta M' = 0, \quad (28b)$$

$$M' - 4\pi r^2 \rho = 0. \quad (28c)$$

Eqs. (28a) and (28b) only explicitly depend on the unknowns E , M , and inherently on Λ , while all the other quantities as for instance ρ , are completely defined by giving these two functions. Therefore, the system is reduced to the two former equations.

The initial data in Eqs.(23) should be rewritten as a proper set of Cauchy data, that is, initial values for $M(t_0, r)$ and $E(t_0, r)$. For $M(t_0, r)$ we trivially obtain from Eq. (28c):

$$M(t_0, r) = 4\pi \int_0^r \rho(t_0, s) s^2 ds. \quad (29)$$

In order to find $E(t_0, r)$, we use $\dot{\rho}(t_0, r)$ to write:

$$\dot{M}_0(r) \equiv 4\pi \int_0^r \dot{\rho}(t_0, s) s^2 ds, \quad (30)$$

and consistently with Eq. (28b), $\dot{M}_0(r) = \dot{M}(t_0, r)$, implies for $E(t_0, r)$ (assuming no initial region of dust vacuum, i.e. $\forall r, M'(t_0, r) \neq 0$), from (22):

$$E(t_0, r) = \left(\frac{\dot{M}_0}{M'(t_0, r)} \right)^2 - \frac{2M(t_0, r)}{r} - \frac{\Lambda r^2}{3}, \quad (31)$$

which means that giving $M(t_0, r), E(t_0, r)$ is equivalent to giving $\rho(t_0, r), \dot{\rho}(t_0, r)$ at the initial surface. The system is now a quasi-linear, first order system, given by

$$\dot{X} = -\beta X' \quad (32a)$$

$$X(t_0, r) = X_0(r), \quad (32b)$$

where

$$X \equiv \begin{bmatrix} E(t, r) \\ M(t, r) \end{bmatrix}. \quad (33)$$

Since the derivative in the normal direction to the initial Cauchy surface is \dot{X} , which is completely determined in terms of X' from the initial surface, the system (32), together with the Cauchy data (33) is well posed.

We further look for the characteristic curves (CCs) of the system [for the method of characteristics see 40]. They can be defined as the integral curves of the coordinates for which the system of PDE's is reduced to a system of ODE's of the form

$$\frac{dX}{ds} = 0. \quad (34)$$

This form implies

$$\frac{\partial}{\partial s} = \partial_t + \beta \partial_r \quad (35)$$

which means that s is just the known Lemaitre-Tolman-Bondi proper time coordinate [1, 24, 30, 41, 42]. Note also that $(\partial_s)^a = n^a$ which means that the CCs correspond to the flow lines. Since the equation is homogeneous, the solution is given by the propagation of the initial values $M(t_0, r)$ and $E(t_0, r)$ along the integral curves of ∂_s .

At the MTS surface separating collapse and expansion $\beta = 0$, and the CC is locally tangent to ∂_t . This condition is equivalent to the turnaround radius condition $\mathcal{L}_n r = 0$ [1], which means that the areal radial velocity of the fluid vanishes at that event. In other words, the surface of this sphere of fluid is instantaneously constant.

We compute the time derivative of β :

$$\dot{\beta} = -\frac{M}{r^2} + \frac{\Lambda r}{3} - \beta \beta', \quad (36)$$

which implies that

$$\frac{d\beta}{ds} = \mathcal{L}_n \beta = \dot{\beta} + \beta \beta' = -\left(\frac{M}{r^2} - \frac{\Lambda r}{3}\right) = -g_{\text{TOV}}, \quad (37)$$

which can be interpreted as the areal radial acceleration of a flow line.

We are naturally interested in MTS surfaces where the areal radial velocity and acceleration vanish. On such a sphere, $\partial_s = \partial_t$. Given an initial condition with $\beta(t_0, r^*) = 0$ and $\dot{\beta}(t_0, r^*) = 0$ at some $t = t_0$ surface $r = r^* > 0$, as the second time derivative reads

$$\ddot{\beta} = -\beta \left[-\frac{M'}{r^2} + \dot{\beta}' \right] - \dot{\beta} \beta', \quad (38)$$

it will vanish on that sphere. This implies that $\beta(t, r^*) = \dot{\beta}(t, r^*) = 0$ for all $t > t_0$, and the sphere will therefore remain unchanged along the fluid evolution.

This result justifies the definition of matter trapping shells/surfaces (MTS's), for the dust+ Λ model.

D. The MTS as the characteristic surface for the dust with Λ model

Consider now the Cauchy problem that consists in solving the system Eqs. (28) using the Cauchy surface of the type $r = r^*$, with boundary conditions matching the MTS conditions, instead of the previous Cauchy surface of the type $t = t_0$. By the conditions $\beta = \dot{\beta} = 0$ for the MTS, we obtain, from Eqs. (28a) and (28b), that the system only admits solutions if we impose boundary data of the type

$$E(t, r^*) = E^*, \quad M(t, r^*) = M^*, \quad (39)$$

which means that all quantities are constant at that surface.

This leaves us with the following questions:

1. Can we integrate inwards and outwards from this surface?
2. Do we obtain separation between the inner and outer solutions?

Since this Cauchy surface is a characteristic surface, together with the system Eq. (32), it constitutes a characteristic Cauchy problem, and therefore the answer to the first question is no. This can be seen in detail in the following realization: the initial data binds the values of X and \dot{X} at the Cauchy surface. In order to solve the system we need

to compute the derivatives normal to the Cauchy surface, which in this case means in the ∂_r directions. This implies solving the system for X' :

$$-\beta^{-1} \dot{X} = X'. \quad (40)$$

As, at our Cauchy surface, $\beta = 0$, solving the above system is not possible. This behaviour is typical of characteristic Cauchy problems, where the Cauchy surface coincides with a CC. In such case, the data from the boundary surface cannot propagate outside from it. Since this is a characteristic Cauchy problem, we have only two types of solution:

[(i)]

1. no solution, if the Cauchy data is not compatible with the problem's equations.
2. infinite solutions, if it is compatible. In such case, any compatible solution of the PDE system can be glued on each side of the Cauchy surface.

Solution (2) is the answer for our second question. In such case, so long as the Cauchy data remains compatible with the surface values, the interior and exterior solutions may be arbitrary. In other words, the MTS Cauchy boundary determines neither the interior, nor the exterior solution, but it guarantees that they do not depend on each other. If we impose, on the basis of physical intuition, that the functions M and E are continuous (which, from a strictly mathematical viewpoint, is not necessary for a solution to the Cauchy problem), then the MTS can be interpreted in a similar way to the continuous matching of the static spherical star solutions to the surrounding Schwarzschild spacetime. The exterior solution only depends on the interior solution quantities at the matching sphere, in this case through the total (MS) mass and the function E , at $r = r_*$.

In summary, the MTS in the case of a dust plus Λ model acts effectively as a shield that not only bridges different spherically symmetric solutions, but also "protects" each side from the detailed dynamics of the other side. One can think of it as analogous to a thin vacuum [or D-vacuum sphere, 43, as Λ is present] spherical shell, that by the virtue of Birkhoff theorem, can be joined to any pair of interior and exterior solutions, provided the continuity conditions required by GR are met.

III. ILLUSTRATIVE CASES WITH DUST AND A COSMOLOGICAL CONSTANT

The conclusion of the previous section reveals that, so long as we have an MTS in a solution to EFEs in spherical symmetry for a dust and cosmological constant content, it can be matched to any other solution with the same generic conditions. In our previous works, we found such conditions, and in particular the presence of an MTS, in two kinds of solutions: Schwarzschild-de Sitter (SdS, spherical vacuum with Λ) and Lemaître-Tolman-Bondi-de Sitter (LTBdS, spherical inhomogeneous dust with Λ). In order to find the MTS areal radius static shell in a homogeneous Friedman-Lemaître-Robertson-Walker-de Sitter solution, the Einstein static universe must be selected (ES). The general framework for these 3 types of solutions is the LTBdS, and we first recall it.

We then need to characterise the MTS in each of the possible solutions before proposing matching conditions. We start, after the general case, with vacuum, then turn to the ES case, before focusing on the more complex LTBdS. For cosmological likelihood, we choose the outer part of the MTS to be built to asymptote a flat FLRW, while the inner part will follow a classical virialised halo density distribution.

Matching the MTS as a Cauchy surface implies that the PDE variables t and r should remain smooth. This implies the matching MTS should have fixed areal radius. Therefore we will have classes of MTS matchings for each pairs of solutions.

A. MTS in LTB with Λ

From our formulation of Λ CDM LTB in Mimoso et al. [1], the governing equations are

$$\beta^2 = \dot{r}^2 = \frac{2M}{r} + \frac{\Lambda}{3}r^2 + E, \quad (41a)$$

$$\ddot{r} = -\frac{M}{r^2} + \frac{\Lambda}{3}r, \quad (41b)$$

with M and E conserved for each shell without shell crossing. Then, the MTS is defined at

$$E = -\frac{2M}{r} - \frac{\Lambda r^2}{3}, \quad (42a)$$

$$\text{gTOV} \equiv \frac{M}{r^2} - \frac{\Lambda r}{3} = 0. \quad (42b)$$

This leads to an MTS for a given $M(r)$ and $E(r)$ profile if both

$$\ddot{r} = 0 : \quad r_{MTS} = \sqrt[3]{\frac{3M}{\Lambda}}, \quad (43)$$

$$\dot{r} = 0 : \quad E_{MTS} = -(3M)^{\frac{2}{3}} \Lambda^{\frac{1}{3}}. \quad (44)$$

B. MTS in Schwarzschild-de Sitter

In the case of Schwarzschild-de Sitter, the Lemaître form of the metric reads

$$ds^2 = -dT^2 + \left(\frac{2m}{r} + \frac{\Lambda r^2}{3} \right) dR^2 + r^2 d\Omega^2, \quad r = r(T, R), \quad (45)$$

$$dR - dT = \left(\frac{2m}{r} + \frac{\Lambda r^2}{3} \right)^{-\frac{1}{2}} dr, \quad \Rightarrow r(T, R) = \left[\sqrt{6m\Lambda} \sinh \left(\frac{3}{2} \sqrt{\frac{\Lambda}{3}} (R - T) \right) \right]^{\frac{2}{3}} \quad (46)$$

while the GLTB form, derived from Eq. (13) for dust with Λ , adopts that of

$$\beta = \dot{r}, \quad (47)$$

$$ds^2 = -dt^2 + \frac{(r' dr)^2}{1 + E(t, R)} + r^2 d\Omega^2. \quad (48)$$

Therefore identification yields

$$M = m = cst, \quad (49)$$

$$E = 0. \quad (50)$$

In this case the MTS in the sense of ALTB can only be found if $\Lambda \rightarrow 0, r_{MTS} \rightarrow \infty$. However, in vacuum, no flow is predefined and we can consider $\dot{r} = 0$ everywhere for any Λ . In this case we can consider that the no acceleration shell r_{MTS} is an MTS.

C. MTS in Einstein-de Sitter

In the case of Einstein-de Sitter, i.e., FLRW with dust and Λ , we start by writing the line element

$$ds^2 = -dt^2 + a^2 \left(\frac{dR^2}{1 - kR^2} + R^2 d\Omega^2 \right), \quad (51)$$

matching it with the GLTB form (48). Identification in this case yields

$$r = aR \Rightarrow \quad r' = a, \quad (52)$$

$$\frac{a^2}{1 - kR^2} = \frac{(r')^2}{1 + E} = \frac{a^2}{1 + E} \Rightarrow \quad E = -kR^2 = -k \left(\frac{r}{a} \right)^2, \quad (53)$$

$$M' = 4\pi r^2 r' \rho(t) \Rightarrow \quad M = \frac{4\pi}{3} r^3 \rho(t). \quad (54)$$

The MTS conditions then lead to

$$-k \left(\frac{r}{a}\right)^2 = -(4\pi\rho(t))^{\frac{2}{3}} \Lambda^{\frac{1}{3}} r^2 \Leftrightarrow k = (4\pi a^3 \rho(t))^{\frac{2}{3}} \Lambda^{\frac{1}{3}} = cst \Rightarrow \rho(t) = \rho_m(t) \propto a^{-3}, \quad (55)$$

$$r_{MTS} = \sqrt[3]{\frac{4\pi\rho(t)}{\Lambda}} r_{MTS} \Leftrightarrow \rho(t) = \frac{\Lambda}{4\pi} = cst \Rightarrow \Lambda = \Lambda_c = \frac{\kappa}{2} \rho_{m0}, a = a_\star = 1, \quad (56)$$

so we can only have an MTS in the Einstein static universe, which is filled with MTSs. In that case, $k = \Lambda_c$, $M = \frac{\Lambda_c}{3} r^3$, $E = -\Lambda_c r^2$ for any r .

D. Building an MTS in LTB example

In order to obtain an example of MTS separating a virialised structure from a cosmological background, we focus on the building of an NFW core with Hubble central flow going to an outward FLRW-like behaviour.

1. The Heaviside MTS jump

We separate the FLRW density behaviour to the outskirts of the central halo. Choosing an inner NFW profile, justified by results of Nbody haloes [44], with cosmological background beyond the MTS

$$\rho = \frac{\rho_0}{\left(\frac{r}{r_0} \left(1 + \frac{r}{r_0}\right)\right)^2} + \rho_b \Theta_H(r - r_{MTS}), \quad (57)$$

where ρ_b is the background energy density recovered for large values of r beyond the MTS radius, ensured by the Heaviside distribution Θ_H , ρ_0 defines the energy density scale of the central halo, and r_0 marks the change of density logarithmic slope from the central cusp $\propto r^{-1}$ to the Keplerian outer decrease as $\propto r^{-3}$. Note that at $r = r_0$, $\rho(r_0) = \frac{\rho_0}{4}$. The corresponding mass then reads

$$M = 4\pi \left\{ r_0^3 \rho_0 \left[\ln \left(1 + \frac{r}{r_0}\right) - \frac{r}{r + r_0} \right] + \rho_b \frac{r^3 - r_{MTS}^3}{3} \Theta_H(r - r_{MTS}) \right\}. \quad (58)$$

At the MTS, the radius is then determined by the scale of Λ , inverting r_{MTS} as $M_{MTS}(r_{MTS}) = \frac{\Lambda}{3} r_{MTS}^3$. This is set by the dynamic condition (41b) with (43). Using the kinematic condition (41a) to ensure that (44) is simultaneously verified leads to having vanishing areal velocity at the MTS.

The dynamic condition determines the position of the MTS by solving

$$M(r) = \frac{\Lambda}{3} r^3 \quad (59)$$

$$\Leftrightarrow \frac{\left(\frac{\Lambda}{4\pi} - \rho_b \Theta_H\right)}{\rho_0} \frac{x^3}{3} + \frac{\rho_b \Theta_H}{\rho_0} \frac{x_0^3}{3} = \ln(1+x) - \frac{x}{x+1}, x = \frac{r}{r_0}, x_0 = \frac{r_{MTS}}{r_0}. \quad (60)$$

Choosing at initial time $t = t_i$, and considering the flat cosmology to set the matter and dark energy components, we get

$$\forall t, \Omega_\Lambda + \Omega_m = 1 \quad \frac{\Lambda}{3} = H_0^2 \Omega_{\Lambda 0} = H_i^2 \Omega_{\Lambda i}, \quad (61)$$

$$\rho_{b0} = \rho_{b i} a_i^3 = \frac{3H_0^2}{8\pi} \Omega_{m0} \Rightarrow H_0^2 \Omega_{m0} = H_i^2 \Omega_{m i} a_i^3, \quad (62)$$

$$\Rightarrow \frac{\Omega_{\Lambda 0}}{\Omega_{m0}} = \frac{\Omega_{\Lambda i}}{(1 - \Omega_{\Lambda i}) a_i^3} \quad \Rightarrow \Omega_{\Lambda i} = \frac{a_i^3 \Omega_{\Lambda 0}}{\Omega_{m0} + a_i^3 \Omega_{\Lambda 0}}. \quad (63)$$

In addition, we have the relation

$$\frac{H_0^2}{H_i^2} = \frac{\Omega_{\Lambda i}}{\Omega_{\Lambda 0}} = \frac{a_i^3}{\Omega_{m0} + a_i^3 \Omega_{\Lambda 0}}. \quad (64)$$

With the choice of the conditions

$$\rho_b \Theta_H = \rho_m \Theta_H (r - r_{MTS}) = \rho_{c,i} \Omega_{m,i} \Theta_H (r - r_{MTS}) = 0 \quad r < r_{MTS}, \quad (65)$$

$$\frac{\Lambda}{4\pi} = 2\rho_\Lambda = 2\rho_{c,i} \Omega_{\Lambda,i}, \quad (66)$$

the constraint (59) constraint then becomes

$$\frac{\rho_c}{\rho_0} (2\Omega_\Lambda) \frac{x^3}{3} = \frac{\rho_c}{\rho_0} \frac{2a_i^3 \Omega_{\Lambda_0}}{\Omega_{m,0} + a_i^3 \Omega_{\Lambda_0}} \frac{x^3}{3} = \ln(1+x) - \frac{x}{x+1}, \quad (67)$$

which admits one nonzero solution. For example, choosing

$$\Omega_{\Lambda_0} = 0.7, \quad \Omega_{m,0} = 0.3, \quad a_i = 10^{-2}, \quad \rho_0 = 200\rho_c, \quad (68)$$

the numerical solution to

$$\frac{a_i^3 \Omega_{\Lambda_0}}{\Omega_{m,0}} - \frac{3\rho_0}{2\rho_c x^3} \left(\ln(1+x) - \frac{x}{x+1} \right) \simeq 0, \quad (69)$$

yields $\frac{r_{MTS}}{r_0} = x_0 \simeq 907.5$.

2. Smooth cosmological transition

In fact we may want a smoother cut off than the Heaviside distribution.

a. Induced initial time limit The small, finite value of the Heaviside replacement at the MTS imposes that the initial time occurs after a cutoff time as deduced below in a simple approximation.

If we still want the above approximation to be correct at initial time a_i , we can impose a condition on the value of the smooth function modeled as a constant T_H , as

$$\frac{2\Omega_{\Lambda,i}}{T_H \Omega_{m,i}} = \frac{2}{T_H} \frac{\Omega_{\Lambda,0}}{\Omega_{m,0}} a_i^3 \simeq 10^h \quad (70)$$

$$\Leftrightarrow T_H = \frac{2\Omega_{\Lambda,0}}{\Omega_{m,0}} a_i^3 10^{-h} = \frac{14}{3} 10^{-h-6} \quad (71)$$

then the existence of a solution to the constraint (59) is leading to

$$2\rho_\Lambda - \rho_b = \rho_{c,i} (2\Omega_{\Lambda,i} - T_H \Omega_{m,i}) > 0 \quad (72)$$

$$\Leftrightarrow 2\Omega_{\Lambda,i} - T_H \Omega_{m,i} = \frac{2a_i^3 \Omega_{\Lambda,0} - T_H \Omega_{m,0} (\Omega_{m,0} a_i^{-3} + \Omega_{\Lambda,0})}{\Omega_{m,0} + a_i^3 \Omega_{\Lambda,0}} > 0 \quad (73)$$

$$\Leftrightarrow a_i^6 - T_H \frac{\Omega_{m,0}}{2} a_i^3 - T_H \frac{\Omega_{m,0}^2}{2\Omega_{\Lambda,0}} = \left(a_i^3 - T_H \frac{\Omega_{m,0}}{4} \right)^2 - T_H \frac{\Omega_{m,0}^2}{2\Omega_{\Lambda,0}} - \left(T_H \frac{\Omega_{m,0}}{4} \right)^2 > 0 \quad (74)$$

$$\Rightarrow a_i^3 > \sqrt{T_H} \left(\sqrt{T_H} \frac{\Omega_{m,0}}{4} + \sqrt{\frac{\Omega_{m,0}^2}{2\Omega_{\Lambda,0}} + T_H \left(\frac{\Omega_{m,0}}{4} \right)^2} \right) = a_{i,\min}^3 \simeq \Omega_{m,0} \sqrt{\frac{T_H}{2\Omega_{\Lambda,0}}} \quad (75)$$

$$\Rightarrow a_i > \left(\Omega_{m,0} \sqrt{\frac{T_H}{2\Omega_{\Lambda,0}}} \right)^{\frac{1}{3}} = \sqrt{a_i} 10^{-\frac{h}{6}} \Omega_{m,0}^{\frac{1}{6}} \simeq a_{i,\min} \quad (76)$$

$$\Rightarrow h > 6 - \log(\Omega_{m,0}) \simeq 6.52. \quad (77)$$

If we choose $h = 7$, we get

$$T_H = 4.67 \times 10^{-13} \quad (78)$$

$$a_{i,\min} \simeq 8.33 \times 10^{-3}, \quad (79)$$

so the MTS only exists after some evolution of the background cosmology. In fact, as ρ_b decreases with cosmological

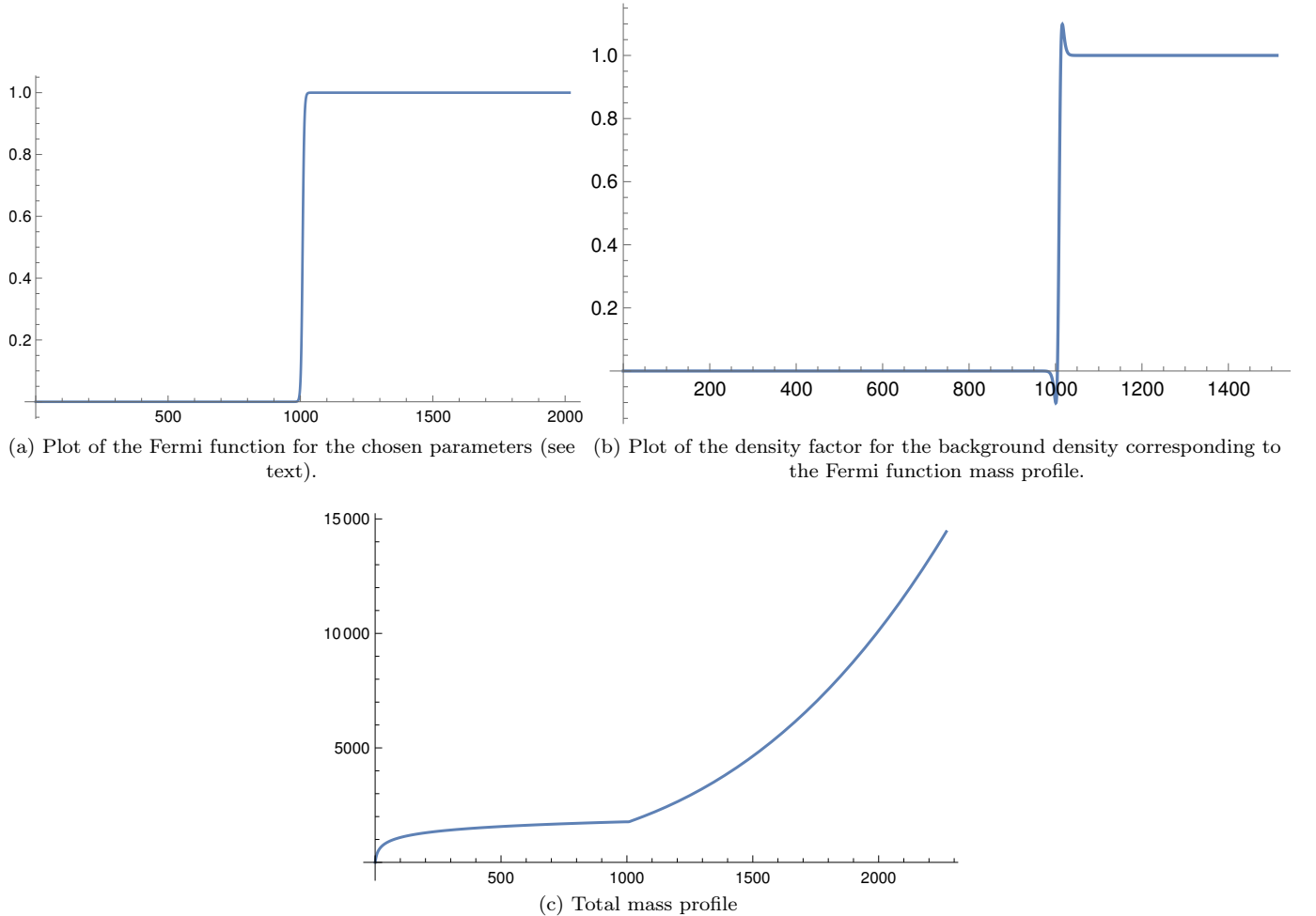


Figure 1: Mass determination with smooth transition

evolution, the real cutoff is probably closer to our choice of a_i .

b. Smoother function If we want to use a smoother function instead of Θ_H , we can choose a type of sigmoid function, namely the Fermi function, for the mass and derive it to get the density. We choose to dissociate the MTS from the transition location at x_T so as to get a controlled, small value of the function and use the above approximation to ensure a similar cutoff time.

$$\begin{aligned} \Theta_H(x - x_T) \text{ in } M \rightarrow & F_H\left(x = \frac{r}{r_0}, k\right) = \frac{1}{1 + e^{-k(x-x_T)}}, \\ \Theta_H(x - x_T) \text{ in } \rho \rightarrow & f_H(x) = \frac{[(x^3 - x_T^3) F_H]'}{3x^2} = F_H(x, k) \left[1 + k \frac{(x^3 - x_T^3)}{3x^2} e^{-k(x-x_T)} F_H(x, k) \right]. \end{aligned}$$

They are plotted in Figs. 1a and 1b, for the choice $x_T = \frac{x_0}{\alpha}$, $\alpha = 0.9$ and $k = 0.32$. This choice ensures that $|F_H(x)| \underset{x \lesssim x_0}{\lesssim} 9.70 \times 10^{-15} < T_H$ for $x < x_0$, so the approximations for the determination of x_0 are secured. The new

mass, plotted in Fig. 1c, and density functions then read, using the previous prescriptions,

$$\begin{aligned} M &= H_i^2 r_0^3 \left\{ 300 \left[\ln(1+x) - \frac{x}{1+x} \right] + \frac{H_0^2}{2H_i^2} \Omega_{m0} a_i^{-3} (x^3 - x_T^3) F_H(x) \right\} \\ &= H_i^2 r_0^3 \left\{ 300 \left[\ln(1+x) - \frac{x}{1+x} \right] + \frac{1}{2} \frac{\Omega_{m0}}{\Omega_{m0} + a_i^3 \Omega_{\Lambda0}} (x^3 - x_T^3) F_H(x) \right\}, \end{aligned} \quad (80)$$

$$\begin{aligned} \rho &= \frac{M'}{4\pi r_0^2 x^2} = \frac{H_i^2 r_0}{4\pi} \left\{ 300 \left[\frac{1}{x(1+x)^2} \right] + \frac{3H_0^2}{2H_i^2} \Omega_{m0} a_i^{-3} f_H(x) \right\} \\ &= \frac{H_i^2 r_0}{4\pi} \left\{ 300 \left[\frac{1}{x(1+x)^2} \right] + \frac{3}{2} \frac{\Omega_{m0}}{\Omega_{m0} + a_i^3 \Omega_{\Lambda0}} f_H(x) \right\}. \end{aligned} \quad (81)$$

3. Kinematic profile condition

The kinematic condition just requires an areal velocity profile that ensures $\dot{r} = 0$ at the MTS. We opt for a Hubble behaviour near the centre and at infinity to meet the standard cosmological framework.

Note that the Hubble parameter value need not be the same on each side of the MTS as they both can yield the $\dot{r} = 0$ condition. Samely the mass profile inside and outside the MTS can differ so long as they yield the same density and mass at the MTS.

The MTS condition suggests an $(r - r_{MTS})^2$ factor to ensure both MTS condition and infinity Hubble-type velocity. An additional factor of $\tanh^2\left(\frac{r}{r_{MTS}}\right)$ ensures Hubble behaviour in the centre. Defining $H_{i\text{in}}^2 = H_i^2 q$ and $H_{i\text{out}}^2 = H_i^2$, we can then propose the areal velocity profile

$$\dot{r}^2 = H_i^2 (q \Theta_H(x_0 - x) + \Theta_H(x - x_0)) r_0^2 \tanh^2\left(\frac{x}{x_0}\right) (x - x_0)^2. \quad (82)$$

As the MTS setting is independent of the Hubble parameter value, we can again approximate the shifted Heaviside distribution with $F_H(x, k)$, maintaining the position of the MTS at x_0 so the velocity profile can be written

$$\dot{r}^2 = H_i^2 (q F_H(x, -k) + F_H(x, k)) r_0^2 \tanh^2\left(\frac{x}{x_0}\right) (x - x_0)^2. \quad (83)$$

The choice of q follows from ensuring the E profile (41a) only intersects the E_{MTS} profile (44) at the MTS (and possibly at the origin), leading to inner trapped shells below the MTS so no shell crossing can occur [1], as opposed to [2]. Noting $e \equiv \frac{E}{x^2 r_0^2 H_i^2}$, $m \equiv \frac{M}{x^3 r_0^3 H_i^2}$, $\dot{\chi}^2 \equiv \frac{\dot{x}^2}{H_i^2 x^2}$, $\frac{\Lambda}{3} = H_i^2 \Omega_{\Lambda i}$ and $e_M \equiv \frac{E_{MTS}}{x^2 r_0^2 H_i^2}$, Eqs. (41a) and (44) lead to

$$e = \dot{\chi}^2 - 2m - \Omega_{\Lambda i}, \quad (84a)$$

$$e_M = -3m^{\frac{2}{3}} \Omega_{\Lambda i}^{\frac{1}{3}}. \quad (84b)$$

Thus the constraint $E < E_{MTS}$ for $x < x_0$, with the values

$$\begin{aligned} m &= \frac{300}{x^3} \left[\ln(1+x) - \frac{x}{1+x} \right] + \frac{1}{2} \frac{\Omega_{m0}}{\Omega_{m0} + a_i^3 \Omega_{\Lambda0}} \left(1 - \left(\frac{x_T}{x} \right)^3 \right) F_H(x) \\ &\underset{x < x_0}{\simeq} \frac{300}{x^3} \left[\ln(1+x) - \frac{x}{1+x} \right], \end{aligned} \quad (85a)$$

$$\dot{\chi}^2 = (q F_H(x, -k) + F_H(x, k)) \tanh^2\left(\frac{x}{x_0}\right) \left(1 - \frac{x_0}{x}\right)^2 \underset{x < x_0}{\simeq} q \tanh^2\left(\frac{x}{x_0}\right) \left(1 - \frac{x_0}{x}\right)^2, \quad (85b)$$

leads to

$$\frac{E_{MTS} - E}{x^2 r_0^2 H_i^2} > 0 \Leftrightarrow \Delta e_W(x) = 2m + \Omega_{\Lambda i} - 3m^{\frac{2}{3}} \Omega_{\Lambda i}^{\frac{1}{3}} > \dot{\chi}^2 = K(x) \geq 0. \quad (86)$$

Plotting $\Delta e_W(x)$ reveals that it is strictly positive, except at x_0 . This restricts the interior Hubble parameter, as

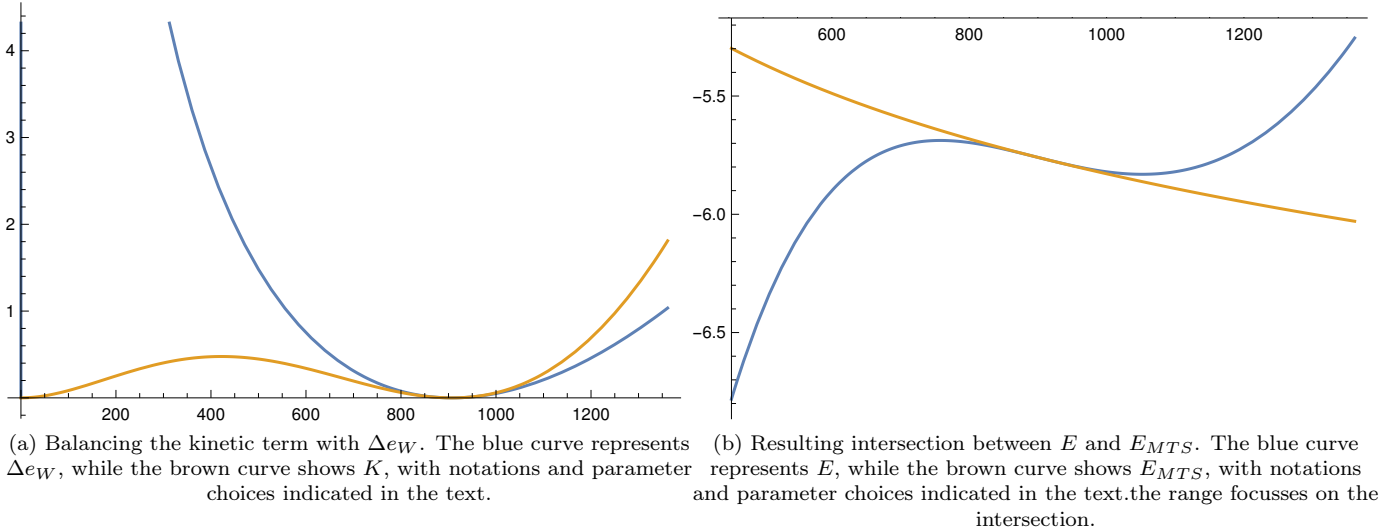


Figure 2: Adjusting inner Hubble parameter to the no-shell-crossing condition.

observable	ρ	M	E	Λ	r_{MTS}
SdS	0	m	0	Λ	$\sqrt[3]{\frac{3m}{\Lambda}}$
ES	$\frac{M'}{4\pi r^2 r'} = \rho_{m0}$	$\frac{\Lambda_c}{3} r^3$	$-\Lambda_c r^2$	$\Lambda_c = 4\pi \rho_{m0}$	$\forall r \Rightarrow r = \sqrt[3]{\frac{3m}{\Lambda}}$
SdS to ES jump at r_{MTS}	$\Delta\rho = \rho_{m0}$	$\Delta M = \left(\frac{\Lambda_c}{\Lambda} - 1\right) m$	$\Delta E = -\Lambda_c r_{MTS}^2$	$\Delta\Lambda = \Lambda_c - \Lambda$	0

Table I: SdS–ES junction

Δe_W is tangent to the horizontal at x_0 , since

$$\Delta e_W(x_0) = 0, \quad \Delta e'_W(x_0) = 0, \quad \Delta e''_W(x_0) = 6\Omega_{\Lambda_i} \left(\frac{100}{x_0^2(1+x_0)^2} - \frac{\Omega_{\Lambda_i}}{x_0} \right)^2 \simeq 1.51 \times 10^{-11}, \quad (87)$$

while the kinetic term yields

$$K(x_0) = 0, \quad K'(x_0) = 0, \quad K''(x_0) = 2q \left(\frac{\tanh(1)}{x_0} \right)^2 \simeq 1.41 \times 10^{-6} q. \quad (88)$$

In the range $x < x_0$ in this case, to ensure no intersection before x_0 , we can choose $\frac{K''(x_0)}{\Delta e''_W(x_0)} \leq 1 \Rightarrow q \leq q_{max} \simeq 1.07 \times 10^{-5}$. The q_{max} choice avoids further shell crossings outside of x_0 , so we adopt it in Fig. 2a. This approximate no-shell-crossing condition leads to $E < E_{MTS}$ for $x < x_0$, while $E > E_{MTS}$ for $x > x_0$, as illustrated in Fig. 2b. Then the corresponding E and E_{MTS} profiles are obtained.

4. Total E and E_{MTS} profiles

The GLTB model is then determined by the total mass and velocity profiles (80) and (83), inputted in E and E_{MTS} in Eq. (44) and

$$E = H_i^2 r_0^2 \left((qF_H(x, -k) + F_H(x, k)) \tanh^2 \left(\frac{x}{x_0} \right) (x - x_0)^2 - \frac{600}{x} \left[\ln(1 + x) - \frac{x}{1 + x} \right] \right. \\ \left. - \frac{\Omega_{m0}}{\Omega_{m0} + a_i^3 \Omega_{\Lambda0}} x^2 - \frac{\Omega_{m0}}{\Omega_{m0} + a_i^3 \Omega_{\Lambda0}} (x^3 - x_T^3) \frac{F_H(x)}{x} x^2 \right). \quad (89)$$

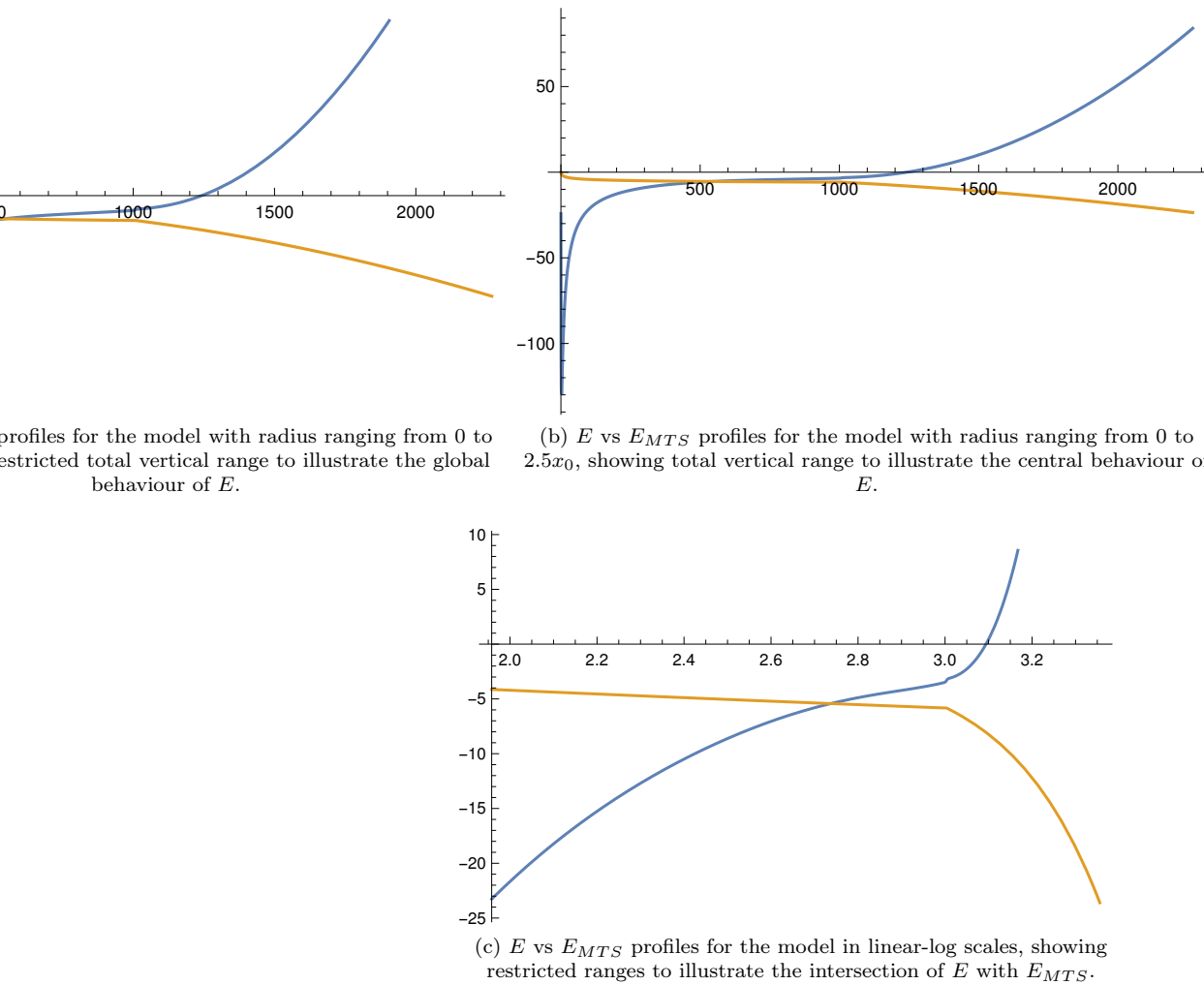


Figure 3: GLTB model with NFW inner halo and FLRW outer behaviour containing a stable MTS. The velocity jump is restricted to a factor 5 for illustration.

Given the value of q defined above, the jump in velocity makes it numerically overwhelming passed the MTS so we represent the total profiles with a jump reduced to a factor 5 for illustration purpose. This allows for a representation of the total model In Fig. 3.

E. MTS as Matching surface between different spacetimes

Armed with the models above, we can produce matching between the three different models studied, Schwarzschild-de Sitter (SdS), Einstein-static (ES) and ALTB (LTBdS), generating 6 different models designated as "inner spacetime"–"outer spacetime": SdS–ES, SdS–LTBdS, ES–SdS, ES–LTBdS, LTBdS–SdS, and LTBdS–ES.

1. SdS–ES and ES–SdS

In the first case we have a vacuum sphere surrounded by a static dust, while the second case surrounds a central static dust ball by vacuum. Separation is made at the MTS for the same continuous $r = r_{MTS}$. However the mass, curvature and cosmological constant need not be continuous at the MTS. This is illustrated in Table I.

observable	ρ	M	E	Λ	r_{MTS}
SdS	0	m	0	Λ_{SdS}	$\sqrt[3]{\frac{3m}{\Lambda_{SdS}}}$
LTBdS	$\rho = \text{Eq. (81)}$	$M = \text{Eq. (80)}$	$E = \text{Eq. (89)}$	$\Lambda = 3H_i^2\Omega_{\Lambda_i}$	$x_0r_0 \Rightarrow r_0 = \sqrt[3]{\frac{3m}{\Lambda_{SdS}x_0^3}}$
ES to LTBdS jump at r_{MTS}	$\Delta\rho = \rho_{m0}$	$\Delta M = \frac{\Lambda x_0}{\sqrt[3]{3m^2\Lambda_{SdS}^2}} - m$	$\Delta E = -H_i^2\sqrt[3]{\frac{9m^2}{\Lambda_{SdS}^2}}$	$\Delta\Lambda = 3H_i^2\Omega_{\Lambda_i} - \Lambda_{SdS}$	0

Table II: SdS–LTBdS junction

observable	ρ	M	E	Λ	r_{MTS}
ES	$\frac{M'}{4\pi r^2 r'} = \rho_{m0}$	$\frac{\Lambda_c}{3}r^3$	$-\Lambda_c r^2$	$\Lambda_c = 4\pi\rho_{m0}$	$\forall r$
LTBdS	$\rho = \text{Eq. (81)}$	$M = \text{Eq. (80)}$	$E = \text{Eq. (89)}$	$\Lambda = 3H_i^2\Omega_{\Lambda_i}$	x_0r_0
ES to LTBdS jump at r_{MTS}	$\Delta\rho = 0$	$\Delta M = \left(\frac{\Lambda}{r_0} - \Lambda_c\right)\frac{r_{MTS}^3}{3}$	$\Delta E = (\Lambda_c - H_i^2)r_{MTS}^2$	$\Delta\Lambda = 3H_i^2\Omega_{\Lambda_i} - 4\pi\rho_{m0}$	0

Table III: ES–LTBdS junction

2. SdS–LTBdS and LTBdS–SdS

In the first case we have a vacuum sphere surrounded by an expanding dust LTBdS, while the second presents the collapsing core of the LTBdS surrounded by vacuum. The continuous radial separation is determined this time by the static MTS of the LTBdS side, at $r_{MTS} = x_0r_0$. Again, the mass, curvature and cosmological constant need not be continuous, as shown in Table II.

3. ES–LTBdS and LTBdS–ES

In the first case, a central static dust ball is surrounded by an expanding dust LTBdS, while the second illustrates a collapsing core of the LTBdS surrounded by a static dust environment. The continuous spatial separation at the MTS is set by the choice of NFW scale r_0 . As in previous cases, the mass, curvature and cosmological constant need not be continuous, as shown in Table III.

IV. CONCLUSION

In this paper, we have rigorously examined Matter Trapping Surfaces (MTS) within the framework of cosmology and gravitation by formulating the problem as a Cauchy problem for dust with a cosmological constant (Λ). Our main result is the establishment that MTSs are characteristic surfaces of the Cauchy problem, generated by the characteristic curves of the PDE system. This implies two possible outcomes: either there is no solution to the Cauchy problem, or there are infinite solutions. In the latter case, any solution to the partial differential equation (PDE) system on one side of the MTS can be extended to either side of the MTS.

To illustrate the effects of this proposition, we presented three examples containing MTSs—Einstein-static (ES), Schwarzschild-de Sitter (SdS), and Lemaître-Tolman-Bondi-de Sitter (LTBdS) models—forming six combinations of solutions. Specifically, we developed an LTBdS model with a central Navarro-Frenk-White (NFW) profile and a Heaviside-limited FLRW-like expanding outer region. These examples demonstrate the practical application of the mathematical properties we found and show that the LTBdS model can present a static, stable MTS for the first time.

The implications of these findings are significant. By showing that MTSs can be used to glue different solutions on either side, our work provides a powerful tool for constructing and analyzing complex cosmological models. This approach not only advances theoretical understanding but also offers a robust method for modeling matter distribution and dynamics in the universe.

In addition, this result strengthens the interpretation of the MTS as the separating shell between expanding and collapsing regions. For a Λ CDM matter model the separation is even sharper, since the MTS acts as a boundary beyond which no detailed information about the dynamic flow in the interior propagates to the exterior, and vice versa. This makes it possible to match any interior and exterior solutions that satisfy the minimal physical conditions required to be interpreted as a spacetime. In this sense, the result is reminiscent of the situation in which, by virtue of

Birkhoff's theorem, one may join any interior Schwarzschild solution to the exterior vacuum Schwarzschild spacetime provided they share the same mass and areal radius at the junction surface.

Following these results, a natural question is whether this MTS separation effect also persists in models with non-zero pressure, where the dynamics become substantially more intricate. It is also worth emphasizing that the present analysis assumes strict spherical symmetry. Therefore, a natural extension would be to incorporate angular momentum in the dust shells and to explore alternative symmetry classes.

In conclusion, our study establishes a solid foundation for the use of MTSs in cosmology and gravitation, offering new pathways for research and practical applications. The ability to generate and utilize stable MTSs in various cosmological scenarios opens up significant opportunities for advancing our understanding of the universe's structure and evolution.

ACKNOWLEDGMENTS

MLED acknowledges the financial support by the Lanzhou University starting fund, the Fundamental Research Funds for the Central Universities (Grants No. lzujbky-2019-25 and lzujbky-2025-jdzx07), the Natural Science Foundation of Gansu Province (No. 22JR5RA389 and No.25JRRA799), National Science Foundation of China (NSFC grant No.12247101)and the '111 Center' under Grant No. B20063.

[1] J. P. Mimoso, M. Le Delliou, and F. C. Mena, *Phys. Rev. D* **81**, 123514 (2010), arXiv:0910.5755 [gr-qc].
[2] M. Le Delliou, F. C. Mena, and J. P. Mimoso, *Phys. Rev. D* **83**, 103528 (2011), arXiv:1103.0976 [gr-qc].
[3] J. P. Mimoso, M. Le Delliou, and F. C. Mena, *Phys. Rev. D* **88**, 043501 (2013), arXiv:1302.6186 [gr-qc].
[4] Y. Foures-Bruhat, *Acta Mat.* **88**, 141 (1952).
[5] Y. Choquet-Bruhat and R. P. Geroch, *Commun. Math. Phys.* **14**, 329 (1969).
[6] A. Lichnerowicz, *Bull. Soc. Math. Fr.* **72**, 146 (1944).
[7] A. Lichnerowicz, *Journal de Mathématiques Pures et Appliquées 9e série*, **23**, 37 (1944).
[8] S. Deser, *Ann. Inst. H. Poincaré Phys. Theor. A* **7**, 149 (1967).
[9] J. W. York, Jr., *Phys. Rev. Lett.* **26**, 1656 (1971).
[10] J. W. York, Jr., *Phys. Rev. Lett.* **28**, 1082 (1972).
[11] J. W. York, Jr., *J. Math. Phys.* **14**, 456 (1973).
[12] J. W. York, Jr., in *10th Marcel Grossmann Meeting on Recent Developments in Theoretical and Experimental General Relativity*, (2004) pp. 3–16, arXiv:gr-qc/0405005.
[13] A. Komar, *Phys. Rev.* **111**, 1182 (1958).
[14] R. Bartnik and J. Isenberg, in *50 Years of the Cauchy Problem in General Relativity: Summer School on Mathematical Relativity* (2002) arXiv:gr-qc/0405092.
[15] P. T. Chrusciel, J. Isenberg, and D. Pollack, *Commun. Math. Phys.* **257**, 29 (2005), arXiv:gr-qc/0403066.
[16] M. T. Anderson, *Commun. Math. Phys.* **222**, 533 (2001), arXiv:gr-qc/0006042.
[17] H. Ringström, *Class. Quant. Grav.* **32**, 124003 (2015).
[18] J. Isenberg, "The Initial Value Problem in General Relativity," in *Springer Handbook of Spacetime*, edited by A. Ashtekar and V. Petkov (2014) pp. 303–321, arXiv:1304.1960 [gr-qc].
[19] W. Tichy, *Rept. Prog. Phys.* **80**, 026901 (2017), arXiv:1610.03805 [gr-qc].
[20] E. Gourgoulhon, (2007), arXiv:gr-qc/0703035.
[21] O. Lahav and A. R. Liddle, arXiv e-prints , arXiv:1912.03687 (2019), arXiv:1912.03687 [astro-ph.CO].
[22] C. W. Misner and D. H. Sharp, *Phys. Rev.* **136**, B571 (1964).
[23] R. L. Arnowitt, S. Deser, and C. W. Misner, *Phys. Rev.* **116**, 1322 (1959).
[24] P. D. Lasky and A. W. C. Lun, *Phys. Rev. D* **75**, 024031 (2007), arXiv:gr-qc/0612007 [gr-qc].
[25] R. J. Adler, J. D. Bjorken, P. Chen, and J. S. Liu, *American Journal of Physics* **73**, 1148 (2005), arXiv:gr-qc/0502040.
[26] P. D. Lasky and A. W. C. Lun, *Phys. Rev. D* **74**, 084013 (2006), arXiv:gr-qc/0606055.
[27] P. D. Lasky and A. W. C. Lun, *Phys. Rev. D* **75**, 104010 (2007), arXiv:0704.3634 [gr-qc].
[28] R. Gautreau, *Phys. Rev. D* **29**, 186 (1984).
[29] S. Carroll, *Spacetime and Geometry* (Addison-Wesley Publishing Company, San Francisco, 2004).
[30] R. C. Tolman, *Proc. Natl. Acad. Sci. U.S.A.* **20**, 169 (1934).
[31] J. R. Oppenheimer and G. M. Volkoff, *Phys. Rev.* **55**, 374 (1939).
[32] J. E. Gunn and J. R. Gott, III, *Astrophys. J.* **176**, 1 (1972).
[33] J. A. Fillmore and P. Goldreich, *Astrophys. J.* **281**, 1 (1984).
[34] E. Bertschinger, *Astrophys. J. Suppl.* **58**, 39 (1985).
[35] G. Korkidis, V. Pavlidou, K. Tassis, E. Ntormousi, T. N. Tomaras, and K. Kovlakas, 1912.08216.
[36] A. Del Popolo and M. H. Chan, *Phys. Rev. D* **102**, 123510 (2020), arXiv:2104.12768 [astro-ph.CO].
[37] L. Herrera, *Phys. Lett. A* **165**, 206 (1992).

- [38] A. Di Prisco, E. Fuenmayor, L. Herrera, and V. Varela, [Phys. Lett. A 195, 23 \(1994\)](#).
- [39] A. Di Prisco, L. Herrera, and V. Varela, [Gen. Rel. Grav. 29, 1239 \(1997\)](#).
- [40] R. Courant and D. Hilbert, [Methods of Mathematical Physics, Vol. 2](#) (Wiley-VCH, 1962).
- [41] G. Lemaître, [Annales Soc. Sci. Brux. Ser. A 53, 51 \(1933\)](#), reprinted in [Gen. Relativ. Gravit. 29\(5\), 641–680 \(1997\)](#).
- [42] H. Bondi, [Mon. Not. R. Astron. Soc. 107, 410 \(1947\)](#).
- [43] K. A. Bronnikov, S.-W. Kim, and M. V. Skvortsova, [Classical and Quantum Gravity 33, 195006 \(2016\)](#), arXiv:1604.04905 [gr-qc].
- [44] J. F. Navarro, C. S. Frenk, and S. D. M. White, [Astrophys. J. 462, 563 \(1996\)](#), astro-ph/9508025 [arXiv].